Curve Tracking Control for Legged Locomotion in Horizontal Plane

Fumin Zhang

Department of Mechanical and Aerospace Engineering

Princeton University

{fzhang}@princeton.edu

Abstract— We derive a hybrid feedback control law for the lateral leg spring (LLS) model so that the center of mass of a legged runner follows a curved path in horizontal plane. The control law enables the runner to change the placement and the elasticity of its legs to move in a desired direction. Stable motion along a curved path is achieved using curvature, bearing and relative distance between the runner and the curve as feedback. Constraints on leg parameters determine the class of curves that can be followed. We also derive an optimal control law that stabilizes the orientation of the runner's body relative to the velocity of the runner's center of mass.

I. INTRODUCTION

From tiny ants to large elephants, legged locomotion is the dominant method that animals use to move on the ground. Although the leg structures are vastly different across species, the mechanisms for walking, jumping or running obey strikingly similar principles. These similarities are captured by mathematical models such as the spring-loaded inverted pendulum (SLIP) model, see [1], and the lateral leg spring (LLS) model in [2]–[5]. The LLS model describes motion in the horizontal plane and the SLIP model describes motion in the sagittal (vertical) plane.

We use the LLS model in this paper in designing curve tracking control in the horizontal plane; the runner is modeled as a rigid body with two weightless springs attached to a point in the body called the center of pressure (COP). Each spring represents legs on one side of the body. The COP is usually not coincident with the center of mass (COM). Legged locomotions can be self-stabilized—the running or walking gaits stay close to being periodic under disturbances—without feedback control. As indicated by a recent review [6], the self-stabilized walking and running happen when the runner moves along a straight line.

There are many interests in engineering practice to design and build legged robots which are versatile on rough and uneven terrains. Legged robots are greatly appreciated in applications such as searching and rescuing missions and planet exploration. In most missions, the robots must be able to move along an arbitrary path. Feedback control is needed for tracking curved path as well as stabilizing the periodic gaits.

In this paper, we develop feedback control law for the LLS model so that the COM follows a curved path. The legged locomotion modeled by the LLS model is a hybrid system.

Correspondingly, the tracking control contains a discrete tracking algorithm which guarantees convergence to the desired curve and a continuous law to control the leg parameters of the LLS model. We also develop an optimal control law to stabilize the posture of the rigid body. Section II serves as an introduction to the LLS model. The discrete tracking algorithm is developed in Section III. In Section IV, control laws are developed for the leg parameters to enable the discrete tracking algorithm. The constraints on the parameters and the effects on the tracking behavior are discussed in Section V and a modified continuous control law is introduced to handle the constraints. We then develop an optimal control law to achieve desired posture for the rigid body in Section VI. We provide simulation results in Section VII.

II. MOTION OF THE COM

In the horizontal plane, motion generated by the LLS model starts when the free end of one spring (or leg) is placed at a touchdown point P. At this starting moment, the spring is at its free length η_0. If the COM has a non-zero initial velocity $\mathbf{v}$ that is not perpendicular to the spring, then the spring will be first compressed to a minimum length and later be restored to its free length. This process, starting and ending with the spring at its free length η_0, is called a *stance phase* or simply a *stance*. The COM moves from the starting position to an ending position after a stance. Suppose that mechanical energy is conserved during each stance, then the starting and ending speed of a stance is identical. As shown in Figure 1, the end of one stance serves as the beginning of the next stance with the touchdown point P shifted from one side to the other. This allows us to distinguish left stances from right stances based on which leg is supporting the body.

The rigid body moves forward as a result of switching between left and right stances. As shown in Figure 1, we use $\mathbf{r}_i$, $i = 1, 2, ...$, to denote the position of the COM in a lab fixed coordinate frame at the beginning of the ith stance. We use α_i to denote the angle between the velocity $\mathbf{v}_i$ and the spring at rest. For a right stance, the angle is measured counter-clockwise from the spring to the velocity vector. For a left stance, the angle is measured clockwise from the spring to the velocity vector. Under this convention for measuring angles, α_i has to be within the interval $(0, \pi/2)$ to generate forward locomotion.

We can view $\mathbf{r}_i$ as points on a curve Γ which is formed by straight line segments that connects $\mathbf{r}_{i-1}$ with $\mathbf{r}_i$ for all
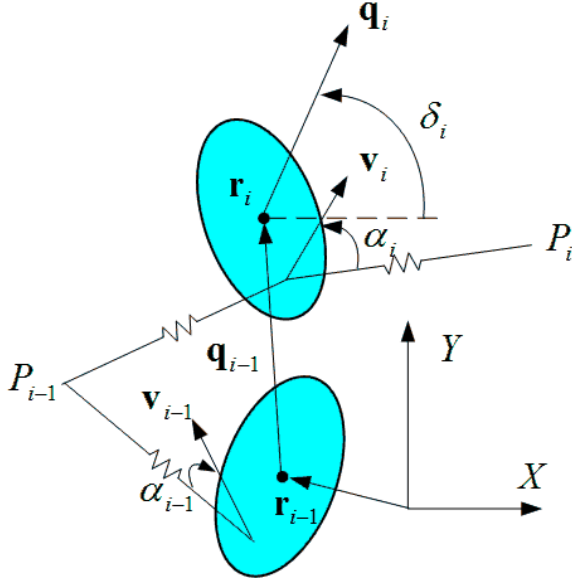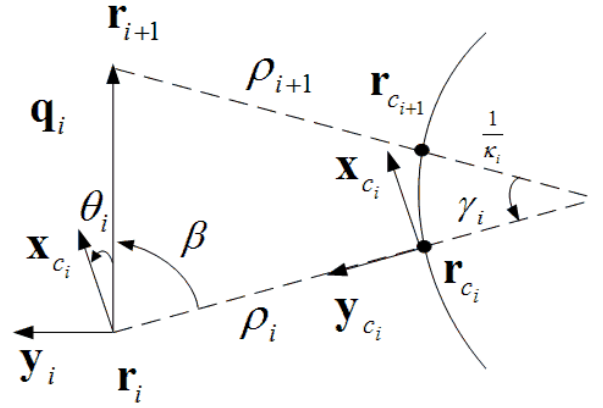
Fig. 2. *The movement of the COM near a boundary curve. θ_i is the angle between $\mathbf{q}_i$ and $\mathbf{x}_{c_i}$. ρ_i is the distance between the COM and the closest point. κ_i is the curvature of the curve. γ_i is the center angle of the arc connecting $\mathbf{r}_{c_i}$ and $\mathbf{r}_{c_{i+1}}$*

Fig. 1. The LLS model for legged locomotion. One left stance followed by one right stance are plotted. The center of mass (COM) is translated from $\mathbf{r}_{i-1}$ to $\mathbf{r}_i$. The velocities of the COM at the beginning of each stance are the vectors $\mathbf{v}_{i-1}$ and $\mathbf{v}_i$. The angle between $\mathbf{v}_i$ and the spring (leg) is α_i. The angle between vector $\mathbf{q}_i$ and the horizontal axis X is δ_i. The positive directions for all angles are as shown.

i. This curve Γ is not the actual trajectory of the COM, but it intersects with the trajectory of the COM at the points $\mathbf{r}_i$. We then let $\mathbf{q}_i = \mathbf{r}_{i+1} - \mathbf{r}_i$ and define $q_i = \| \mathbf{q}_i \|$. We also define an angle δ_i as the angle between the vector $\mathbf{q}_i$ and the horizontal axis of the lab frame, measured counter-clockwise from the axis. This angle describes the direction of curve Γ for the ith stance. The motion of the COM can now be described by a discrete system

$$\mathbf{r}_{i+1} = \mathbf{r}_i + [q_i \cos \delta_i, q_i \sin \delta_i]^T. \tag{1}$$

Next, we develop a boundary tracking algorithm for this discrete system.

III. Tracking a detected boundary

Suppose at the position $\mathbf{r}_i$, the runner is able to detect a segment of a boundary curve from sensor information, c.f., [7] and [8]. Suppose the runner is also able to estimate a point on the boundary curve that has the minimum distance to the COM. We call this point the closest point $\mathbf{r}_{c_i}$ shown in Figure 2. By selecting two extra points on the boundary near $\mathbf{r}_{c_i}$, the runner can estimate the tangent vector to the boundary curve $\mathbf{x}_{c_i}$ and the curvature of the boundary curve κ_i using algorithms summarized in [7]. Here we suppose all estimates are perfect.

We let ρ_i represent the distance between the COM at $\mathbf{r}_i$ and the closest point at $\mathbf{r}_{c_i}$. We also let

$$\mathbf{x}_i = \frac{\mathbf{q}_i}{\| \mathbf{q}_i \|} \tag{2}$$

be the unit vector in the direction of $\mathbf{q}_i$. We can then define two right handed frames—one at $\mathbf{r}_i$ and the other at $\mathbf{r}_{c_i}$—by

defining two unit normal vectors $\mathbf{y}_i$ and $\mathbf{y}_{c_i}$ as shown in Figure 2. The angle θ_i between $\mathbf{x}_i$ and $\mathbf{x}_{c_i}$ is defined by letting

$$\cos \theta_i = \mathbf{x}_i \cdot \mathbf{x}_{c_i} \quad \text{and} \quad \sin \theta_i = -\mathbf{x}_i \cdot \mathbf{y}_{c_i}. \tag{3}$$

In Figure 2, the closest point on the boundary moves from $\mathbf{r}_{c_i}$ to $\mathbf{r}_{c_{i+1}}$ during a stance. We then assume that each stance is short enough so that the curvature of the boundary curve detected during this period can be approximated by a finite constant κ_i. From Figure 2, we observe

$$\beta = \frac{\pi}{2} - \theta_i . \tag{4}$$

Therefore, according to the cosine law, we have

$$(\rho_{i+1} + \frac{1}{\kappa_i})^2 = (\rho_i + \frac{1}{\kappa_i})^2 - 2(\rho_i + \frac{1}{\kappa_i})q_i \sin \theta_i + q_i^2. \tag{5}$$

We can view ρ_i as state variables and consider q_i as the control over step size and θ_i as steering control. Equation (5) describes the controlled relative motion between the COM and the detected boundary curve.

Suppose that the step size q_i has been determined. We need to find θ_i such that ρ_i converges to a desired value ρ_c as $i \rightarrow \infty$. If we can find a feedback control law $f_i(\cdot)$ such that

$$\rho_{i+1} - \rho_i = f_i(\rho_i - \rho_c), \tag{6}$$

then we can choose the function $f_i(\cdot)$ so that $\rho_i - \rho_c \rightarrow 0$. For example, we may let

$$f_i(\rho_i - \rho_c) = -K_i \cdot (\rho_i - \rho_c) \tag{7}$$

where $0 < K_i < 1$. Observe that

$$\rho_{i+1} - \rho_i = \rho_{i+1} - \rho_c - (\rho_i - \rho_c), \tag{8}$$

and this leads to

$$\rho_{i+1} - \rho_c = (1 - K_i)(\rho_i - \rho_c). \tag{9}$$

Since $-1 < 1 - K_i < 1$, it is true that $\rho_i \rightarrow \rho_c$ as $i \rightarrow \infty$.

We now define $\lambda_i = \rho_i + \frac{1}{\kappa_i}$. In order to achieve (6), we replace $(\rho_{i+1} + \frac{1}{\kappa_i})$ with $(\lambda_i + f_i)$ in (5). From (5), we can solve for $\sin\theta_i$ as

$$\begin{aligned}\sin\theta_i &= \frac{-f_i^2 - 2\lambda_i f_i + q_i^2}{2\lambda_i q_i} \\ &= \frac{q_i}{2\lambda_i} - \frac{f_i}{q_i} - \frac{f_i^2}{2\lambda_i q_i}.\end{aligned} \tag{10}$$

When $f_i = 0$, the solution is $\theta_i = \sin^{-1}(q_i/2\lambda_i)$. This corresponds to the runner running parallel to the boundary curve.

Note that when $\kappa_i \to 0$, then $\lambda_i \to \infty$. The limit of equation (10) is

$$\sin\theta_i = -\frac{f_i}{q_i} \tag{11}$$

which is equivalent to $\rho_{i+1} - \rho_i = -q_i \sin\theta_i$. This equation indeed describes the relative motion between the COM and a straight line. Therefore, all the results that will be obtained from (10) are applicable to (11) by letting $\lambda_i \to \infty$.

Lemma 3.1: A solution exists for θ_i in equation (10) if and only if $f_i \in [-(2\lambda_i + q_i), \min\{-q_i, q_i - 2\lambda_i\}]$ or $f_i \in [\max\{-q_i, q_i - 2\lambda_i\}, q_i]$.

Proof: A solution exists for θ_i if and only if

$$\frac{-f_i^2 - 2\lambda_i f_i + q_i^2}{2\lambda_i q_i} \leq 1 \tag{12}$$

and

$$\frac{-f_i^2 - 2\lambda_i f_i + q_i^2}{2\lambda_i q_i} \geq -1. \tag{13}$$

From (12) we have,

$$f_i^2 + 2\lambda_i f_i - (q_i^2 - 2\lambda_i q_i) \geq 0 \tag{14}$$

which is equivalent to

$$(f_i + (2\lambda_i - q_i))(f_i + q_i) \geq 0. \tag{15}$$

This inequality is satisfied if and only if

$$f_i \geq \max\{-q_i, q_i - 2\lambda_i\} \text{ or } f_i \leq \min\{-q_i, q_i - 2\lambda_i\}. \tag{16}$$

From (13) we have,

$$f_i^2 + 2\lambda_i f_i - (q_i^2 + 2\lambda_i q_i) \leq 0 \tag{17}$$

which is equivalent to

$$(f_i + (2\lambda_i + q_i))(f_i - q_i) \leq 0. \tag{18}$$

This inequality is satisfied if and only if

$$-(2\lambda_i + q_i) \leq f_i \leq q_i. \tag{19}$$

Therefore, combining (16) and (19), we have found the necessary and sufficient condition for the existence of solution for θ_i as

$$-(2\lambda_i + q_i) \leq f_i \leq \min\{-q_i, q_i - 2\lambda_i\} \tag{20}$$

or

$$\max\{-q_i, q_i - 2\lambda_i\} \leq f_i \leq q_i. \tag{21}$$

∎

Lemma 3.2: Suppose $0 < q_i < 2\lambda_i$. Let $f_i = -K_i(\rho_i - \rho_c)$. There exists $K_i \in (0, 2)$ such that (21) is satisfied and θ_i in (10) has a solution.

Proof: If $|\rho_i - \rho_c| < \frac{1}{2}\min\{q_i, 2\lambda_i - q_i\}$, we may let K_i be any value in the interval $(0, 2)$ and (21) is satisfied. If $|\rho_i - \rho_c| \geq \frac{1}{2}\min\{q_i, 2\lambda_i - q_i\}$, we may let

$$0 < K_i < \min\{2, \frac{q_i}{|\rho_i - \rho_c|}, \frac{2\lambda_i - q_i}{|\rho_i - \rho_c|}\} \tag{22}$$

which satisfies (21). ∎

The condition $q_i < 2\lambda_i$ in Lemma 3.2 indicates that each step size should not be too big. If the curve has large curvature i.e. small turning radius, then the runner must reduce its step size when being close to the curve. For a straight line, since λ_i is arbitrarily large, there is no constraints on the step size q_i.

Theorem 3.3: Suppose the step size q_i satisfy $0 < q_i < 2\lambda_i$. Let $f_i = -K_i(\rho_i - \rho_c)$. Select $K_i \in (0, 2)$ such that θ_i in (10) has a solution. Then under the control q_i and θ_i, we have $\rho_i \to \rho_c$ as $i \to \infty$.

Proof: Under the selection of q_i, f_i and K_i, we have

$$\rho_{i+1} - \rho_c = (1 - K_i)(\rho_i - \rho_c) \tag{23}$$

for all i. Since $-1 < 1 - K_i < 1$, the convergence is proved. ∎

Once θ_i is determined from (10), we can compute the direction of $\mathbf{q}_i$ in the lab frame. This is because

$$\delta_i = \zeta_i - \theta_i \tag{24}$$

where ζ_i is the angle between the horizontal axis of the lab frame and the vector $\mathbf{x}_{c_i}$, measured counter clockwise from the horizontal axis. Knowing q_i and δ_i allows us to compute the position of the COM for the next stance from the discrete system given by equation (1).

IV. CONTROL THE LLS MODEL

In order to generate desired q_i and δ_i to control the COM movement, the runner needs to change its leg placements or the elasticity of the legs. We investigate the dynamics during each stance to establish the relations between the COM motion and the leg parameters.

Leg parameters for a right stance and a left stance often differ only by the sign. Since a right stance is always followed by a left stance and vice versa, *we use the convention that the stance k is always a right stance and stance $k + 1$ is always a left stance.* Therefore, stance $k + 2$ must be a right stance, etc. In the following, we will only show detailed derivation for a right stance; similar results for a left stance will be listed directly.

We set up a polar coordinate system at the touchdown point P_k with the horizontal x-axis parallel to the horizontal X-axis of the fixed lab frame. Let (η, ψ) be the polar coordinates of the COM in this frame and let σ describe the orientation of the rigid body. Then the total energy is

$$E = \frac{1}{2}m\dot{\eta}^2 + \frac{1}{2}m\eta^2\dot{\psi}^2 + \frac{1}{2}I\dot{\sigma}^2 + V(\eta) \tag{25}$$

where we assume the spring has potential energy V which depends only on its length.

During each stance, the dynamics can be described as a continuous nonlinear Hamiltonian system; the Hamilton equations are developed in [2]. The system is not integrable when the distance between the COM and the COP is nonzero. In this case numerical methods are necessary to compute the trajectory of the COM from knowledge of the states (η, ψ, σ).

To illustrate analytical insights for the tracking problem, it is much easier to study the case when the COP and COM coincide. This is because the corresponding system is integrable. The Hamilton equations for the dynamics of the COM are

$$
\begin{aligned}
p_\eta &= m\dot{\eta} \\
p_\psi &= m\eta^2\dot{\psi} \\
\dot{p}_\eta &= \frac{1}{m\eta^3}p_\psi^2 - \frac{\partial V}{\partial \eta} \\
\dot{p}_\psi &= 0.
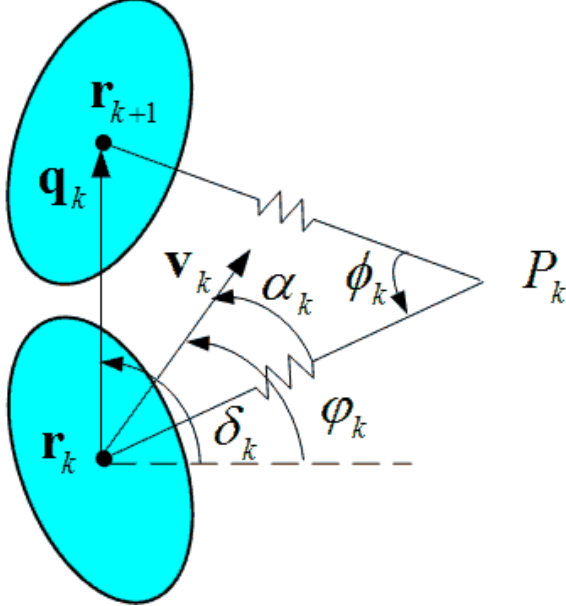\end{aligned}
\tag{26}
$$

Fig. 3. *The LLS model with COM coincide with COP. Angle ϕ_k is the center angle swept during the stance. Angle α_k is the angle between the leg and the velocity $\mathbf{v}_k$ at the moment of touch down.*

We plot one right stance in Figure 3. Let $\mathbf{v}_k$ be the velocity of the COM at the beginning of the kth stance. This $\mathbf{v}_k$ provides initial value for the states p_η and p_ψ of the system (26). Because mechanical energy is conserved, the speed $v_k = \| \mathbf{v}_k \|$ satisfies $v_{k+1} = v_k$. We let α_k represent the angle measured from the leg to the velocity $\mathbf{v}_k$ at the moment of touchdown, and we call α_k *the leg placement parameter*. We use φ_k to measure the direction of velocity in the lab frame. By using simple geometric relationships in Figure 3, we have

$$
\frac{\pi}{2} - \frac{\phi_k}{2} - \alpha_k = \delta_k - \varphi_k.
\tag{27}
$$

Therefore, using equation (24),

$$
\zeta_k - \varphi_k - \theta_k = \frac{\pi}{2} - \alpha_k - \frac{\phi_k}{2}.
\tag{28}
$$

Note that $(\zeta_k - \varphi_k)$ is the relative angle between $\mathbf{v}_k$ and $\mathbf{x}_{c_k}$: the tangent vector to the boundary curve at the closest point. We know θ_k is the angle between vector $\mathbf{q}_k$ and the same tangent vector $\mathbf{x}_{c_k}$. Therefore, $(\zeta_k - \varphi_k - \theta_k)$ is the angle between $\mathbf{v}_k$ and $\mathbf{q}_k$. From (28), we see that changing α_k will change the direction of the COM movement $\mathbf{q}_k$. This is also true for a left stance where we have

$$
\zeta_{k+1} - \varphi_{k+1} - \theta_{k+1} = -(\frac{\pi}{2} - \alpha_{k+1} - \frac{\phi_{k+1}}{2}).
\tag{29}
$$

Another relationship we can derive from Figure 3 is

$$
q_k = 2\eta_k \sin\frac{\phi_k}{2}
\tag{30}
$$

where η_k represents the leg length at the moment of touchdown.

In (30) and (28), q_k is the distance the runner wants to travel in one stance, the angle θ_k can be solved from (10), and the angle $(\zeta_k - \varphi_k)$ is known. We want to solve for the leg parameters α_k and η_k, but ϕ_k is still unknown. This unknown can be solved from the continuous system equations (26).

At the starting position of the kth stance $\mathbf{r}_k$ and the ending position of the kth stance $\mathbf{r}_{k+1}$, by conservation of the angular momentum, we have

$$
p_{\eta_{k+1}} = p_{\eta_k} = \eta_k^2\dot{\psi} = \eta_k v_k \sin\alpha_k.
\tag{31}
$$

Using the method of integration by quadrature, c.f. [9], we can compute the center swing angle ϕ_k for each stance as

$$
\phi_k = 2\int_{\eta_k}^{\eta_{\min}} \frac{\frac{p_{\eta_k}}{\eta^2}}{\pm\sqrt{2E - \frac{p_{\eta_k}^2}{\eta^2} - 2V(\eta)}}d\eta
\tag{32}
$$

where $\eta_{\min}$ is the shortest length of the spring during the stance. When $\eta = \eta_{\min}$, we have $\dot{\eta} = 0$. Thus we can solve $\eta_{\min}$ from

$$
2E - \frac{p_{\eta_k}^2}{\eta_{\min}^2} - 2V(\eta_{\min}) = 0 .
\tag{33}
$$

Explicit formulas can be derived for ϕ_k when we use the linear spring potential $V = b_k(\eta - \eta_k)^2$ where b_k is the spring constant for the kth stance. These formulas require the use of elliptic functions [2].

Since ϕ_k is now a known function of α_k, η_k, and b_k, we can solve for any two of α_k, η_k, and b_k from (28) and (30) when keeping the other parameter constant. For a runner, controlling α_k means to find the appropriate angle between its leg and the direction of the COM motion. On the other hand, as reported by Jindrich and Full in [10], the cockroaches control the length η_k by stretching or compressing their legs when turning. We see that changing η_k will affect both p_{ψ_k} and $V(\eta)$. This changes ϕ_k and hence controls $(\zeta_k - \varphi_k - \theta_k)$. Another means of steering is to change the potential energy $V(\eta)$,e.g., change the spring constant b_k, which also controls ϕ_k.

If the conditions in Theorem 3.3 are satisfied, equation (10) always has a solution for θ_i. The equations (28), (30) and (32) can be solved to implement the control θ_i. We call this method *the inverse method*. Note that finding solutions for α_k and η_k often requires numerical methods because ϕ_k is not a simple function of α_k and η_k.

V. TRACKING BEHAVIOR UNDER CONSTRAINTS

For every stance, the LLS model generates the COM movement $\mathbf{q}_k$ by controlling parameters such as α_k, η_k and b_k. In practice, these parameters all have to be bounded. These bounds post constraints on the possible $\mathbf{q}_k$ that can be generated by the LLS model. In this section, we first discuss the constrained COM movement and investigate the constrained tracking behavior when a runner is running along a curve path. We then derive a new control law with proved convergence under the constraints.

A. the constraints

To generate forward locomotion, the relative angle α_k between the leg and the COM velocity $\mathbf{v}_k$ should be bounded within the interval $(0, \pi/2)$. Figure 4 illustrates the possible $\mathbf{q}_k$ that can be produced by changing α_k for a right stance when η_k and b_k are held constant. The parameters for the plotted LLS model are $m = 2.5$g, $v_k = 0.2$m/s, $\eta_k = 1.7$cm and $b_k = 1.05$N/m which are typical for a cockroach. When $\alpha_k = 0$ and $\alpha_k = \pi/2$, we have $q_k = 0$. Therefore, in order to move forward effectively, the angle α_k must be within an interval $[\alpha_{\min}, \alpha_{\max}]$ with $\alpha_{\min} > 0$ and $\alpha_{\max} < \pi/2$. The solid segment in Figure 4 illustrates the possible $\mathbf{q}_k$ between $\alpha_{\min} = \pi/6$ and $\alpha_{\max} = \pi/3$. We also plot the length q_k as a function of the leg placement angle α_k in Figure 5. There the maximum q_k is 1.44cm. When α_k is within $[\pi/6, \pi/3]$, the minimum q_k is 1.24cm. The changes in q_k is not big for a wide range of α_k. This is typical for LLS models.
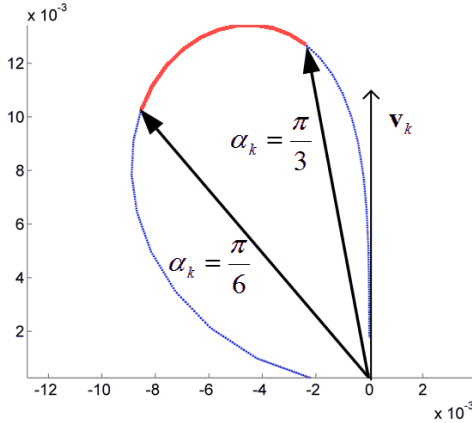

Fig. 4. The possible $\mathbf{q}_k$ generated by a right stance for an LLS model. $\mathbf{v}_k$ is the velocity of the COM. The units are in meters. The curve (dotted and solid) illustrates the end points for vector $\mathbf{q}_k$ starting from the origin when α_k changes from 0 to $\pi/2$ while other parameters are constant. The solid segment corresponds to $\alpha_k \in [\pi/6, \pi/3]$.

The above example suggests that it is possible to keep η_k, q_k and ϕ_k constant for each stance. We control the spring constant b_k and the leg placement angle α_k. The advantage of this strategy is that the distance traveled by the COM is identical for every stance. This fact can help us analyze the tracking behavior later. For the LLS model plotted in Figure 4 and 5, in order to keep $q_k = 1.44$cm, we plot the spring constant b_k as a function of the leg placement angle α_k in
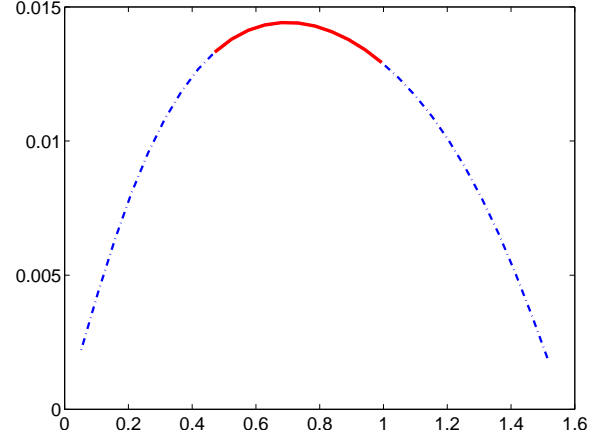

Fig. 5. The length q_k (in meters) traveled by the COM during a right stance for an LLS model as a function of leg placement angle α_k (in radians). The solid segment corresponds to $\alpha_k \in [\pi/6, \pi/3]$.
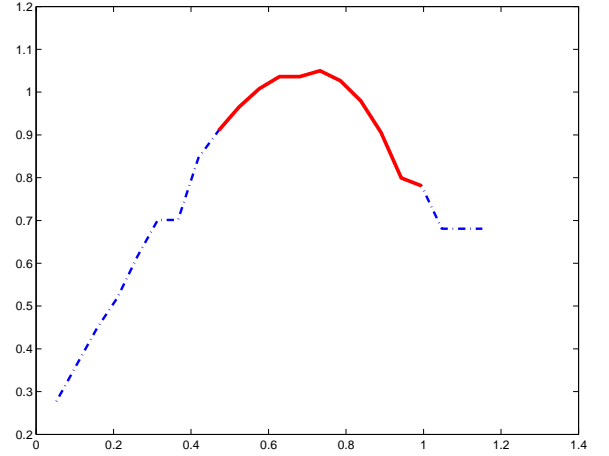

Fig. 6. The spring constant b_k (in N/m) as a function of leg placement angle α_k (in radians) to keep $q_k = 1.44$ cm. The solid segment corresponds to $\alpha_k \in [\pi/6, \pi/3]$.

Figure 6. For $\alpha_k \in [\pi/6, \pi/3]$, b_k lies between 0.78 N/m and 1.06 N/m. This range is not difficult to implement.

With q_k constant for each stance, the possible movement of the COM can be depicted by a cone $\mathcal{C}_k$. The two edges of the cone correspond to $\alpha_k = \alpha_{\min}$ and $\alpha_k = \alpha_{\max}$. The length of both edges are q_k. Figure 7 illustrates cone $\mathcal{C}_{k+1}$ and cone $\mathcal{C}_k$. $\mathcal{C}_{k+1}$ grows from the end point of $\mathbf{q}_k$ which lies in the circular arc of $\mathcal{C}_k$. We found that $\mathcal{C}_{k+1}$ is the mirror image of $\mathcal{C}_k$ with $\mathbf{q}_k$ being the axis of symmetry. This is because the velocity vector $\mathbf{v}_{k+1}$ and $\mathbf{v}_k$ are symmetric with respect to $\mathbf{q}_k$, which can be proved by solving equations (26). Therefore, as the runner moves forward, the cone will flip from side to side.

B. running along a curve path and robustness

We use the index i for all right and left stances. When running parallel to a desired curved path, the COM movement satisfies $\rho_i = \rho_c$ for all i. Therefore, we have $f_i = 0$ in equation (10). The following conditions are necessary:

A1) $\mathbf{q}_i \in \mathcal{C}_i$;
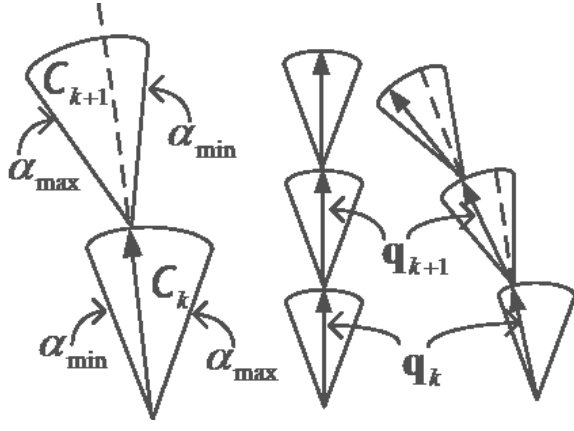A2) $\theta_i = \sin^{-1}(q_i/2\lambda_i)$.

Fig. 7. The cones flip from one side to another when running. On the left, the cones $\mathcal{C}_k$ and $\mathcal{C}_{k+1}$ are symmetric with respect to $\mathbf{q}_k$ which is the solid arrow. In the middle, the runner is running along a straight line. On the right, the runner is running along a curve path in the counter clockwise direction.

Condition A1 requires that the COM movement belongs to the cone that is feasible for the constrained model. Condition A2 requires that $\mathbf{q}_i$ is parallel to the desired curve.
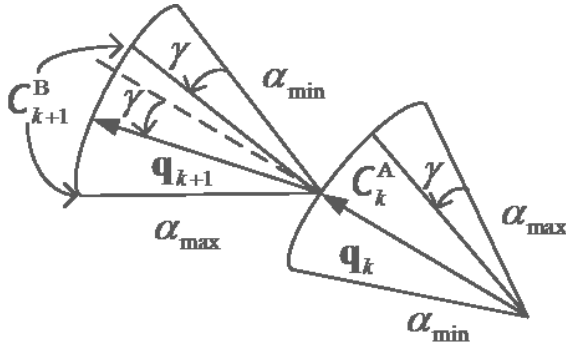

Fig. 8. The sub-cones $\mathcal{C}_k^{\mathrm{A}}$ and $\mathcal{C}_{k+1}^{\mathrm{B}}$. $\mathbf{q}_k$ is the middle line of $\mathcal{C}_k^{\mathrm{A}}$, and $\mathbf{q}_{k+1}$ is the middle line of $\mathcal{C}_k^{\mathrm{A}}$. The angle difference between $\mathbf{q}_{k+1}$ and $\mathbf{q}_k$ is γ.

If the desired curve is a straight line segment, then $\theta_i = 0$ in condition A2. As the runner moving forward, the cone $\mathcal{C}_i$ will be flipping side to side with respect to the straight line. In this case we have $\alpha_i = \alpha_{i+1}$. The robustness of this behavior is determined by the size of the cone and the value of α_i. If we choose the value of α_i so that the COM movement $\mathbf{q}_k$ is always in the middle of the cone, then the tracking behavior is the most robust. See the middle figure in Figure 7.

If the desired curve is convex with positive curvature, then $\theta_i \neq 0$. To find out θ_i, we study the kth and $(k+1)$th stance, i.e., a right stance followed by a left stance. For convenience we let

$$\gamma_k = 2\sin^{-1}\frac{q_k}{2\lambda_k}. \tag{34}$$

From equation (73) in Appendix I and using the fact that $\phi_k = \phi_{k+1}$, we know that θ_k and θ_{k+1} satisfies

$$\theta_{k+1} - \theta_k = -(\alpha_{k+1} - \alpha_k) + \gamma_k. \tag{35}$$

This relation can also be observed from Figure 2. Condition A2 implies that $\theta_{k+1} = \theta_k = \gamma_k/2$. Therefore, when running

along a convex curve, $\alpha_{k+1} - \alpha_k = \gamma_k$ should be satisfied. We have similar relation for stance $k+1$ and $k+2$, i.e., a left stance followed by a right stance: $\alpha_{k+2} - \alpha_{k+1} = -\gamma_{k+1}$. We can then write $\alpha_{i+1} - \alpha_i = \pm\gamma_i$ for all stances. This equation requires that γ_i must be less than $(\alpha_{\max} - \alpha_{\min})$. This implies that λ_i, the instantaneous radius of the curve must satisfy

$$\lambda_i > \frac{q_i}{2\sin\frac{\alpha_{\max}-\alpha_{\min}}{2}}. \tag{36}$$

This condition is stricter than $\lambda_i > q_i/2$ required by Lemma 3.2. Hence the constraint on α_i puts a tighter restriction on the curvature of the curve that can be traced.

We divide $\mathcal{C}_i$ into two sub-cones. Let $\mathcal{C}_i^{\mathrm{A}}$ be the cone for $\alpha \in [\alpha_{\min}, \alpha_{\max} - \gamma_i]$. Let $\mathcal{C}_i^{\mathrm{B}}$ be the cone for $\alpha \in [\alpha_{\min} + \gamma_i, \alpha_{\max}]$. Because $\mathcal{C}_i$ flips and $\alpha_{i+1} - \alpha_i = \pm\gamma_i$, if $\mathbf{q}_i$ belongs to $\mathcal{C}_i^A$, then $\mathbf{q}_{i+1}$ belongs to $\mathcal{C}_{i+1}^B$. Now consider a right stance k followed by a left stance $(k+1)$. When running along a convex curve in the counter clockwise (CCW) direction, the runner must have $\alpha_k \in \mathcal{C}_k^{\mathrm{A}}$ and $\alpha_{k+1} \in \mathcal{C}_{k+1}^{\mathrm{B}}$, see Figure 8. When running in the clockwise (CW) direction, the runner must have $\alpha_k \in \mathcal{C}_k^{\mathrm{B}}$ and $\alpha_{k+1} \in \mathcal{C}_{k+1}^{\mathrm{A}}$.

To increase the robustness of the tracking behavior, we should let the COM movement $\mathbf{q}_i$ be close to the middle of $\mathcal{C}_i$. In the case of convex curves, the best choice is to let $\mathbf{q}_i$ and $\mathbf{q}_{i+1}$ be symmetric with respect to the middle line of $\mathcal{C}_i$. The middle lines of $\mathcal{C}_i^{\mathrm{A}}$ and $\mathcal{C}_i^{\mathrm{B}}$ are symmetric with respect to the middle line of $\mathcal{C}_i$. The angle between the middle lines of $\mathcal{C}_i^{\mathrm{A}}$ and $\mathcal{C}_i^{\mathrm{B}}$ is γ_i. If the curve has constant curvature, then γ_i is constant for all i. This implies that the middle lines of $\mathcal{C}_i^{\mathrm{A}}$ and $\mathcal{C}_{i+1}^{\mathrm{B}}$ are symmetric with respect to the middle line of $\mathcal{C}_i$. Therefore, we may choose $\mathbf{q}_i$ to be the middle line of either $\mathcal{C}_i^{\mathrm{A}}$ or $\mathcal{C}_i^{\mathrm{B}}$ for maximum robustness. If the curve has a changing positive curvature, then γ_i can be different from stance to stance. This "middle line" strategy can not be enforced. In this case one can choose $\mathbf{q}_i$ to be as close to the middle lines as possible.

If the desired curve is not convex, the tracking behavior can be viewed as switching between tracking a locally convex curve in the CCW direction and in the CW direction. The switching depends on how the curve changes from locally convex to locally concave. No general conclusions can be drawn regarding which part of the cone $\mathcal{C}_i$ is used for a stance. In this case the tracking behavior is not a "steady state".

C. The approximation method

The inverse method fails when constrained solutions from (28), (30) and (32) do not exist. We design a new control law that is able to find leg parameters that satisfies all constraints. The control law also guarantees convergence to the desired curve from generic initial conditions. We call this method the *approximation method*.

We investigate the LLS model satisfying $q_i = q$ for all i where q is a positive constant. To keep $q_i = q$, the runner controls both the leg placement angle α_i and the spring parameter b_i. We assume that the desired curve path is either a straight line or a circle i.e. κ_i is constantly κ for all i. This assumption can be relaxed to convex curves with slowly varying curvature. We further assume that the step size q is

much smaller than the radius of the curve path. Under these assumptions, $\rho_{i+1} - \rho_i \ll 2(\rho_i + \frac{1}{\kappa})$, and equation (10) can be simplified to

$$\rho_{i+1} - \rho_{\rm c} = \rho_i - \rho_{\rm c} + \frac{q^2}{2\lambda_i} - q\sin\theta_i \qquad (37)$$

where $\lambda_i = (\rho_i + \frac{1}{\kappa})$. We then view $\sin\theta_i$ as the second state variable other than $\rho_i - \rho_{\rm c}$. It satisfies

$$\sin\theta_i = \sin\left(\zeta_i - \varphi_i \mp (\frac{\pi}{2} - \alpha_i - \frac{\phi_i}{2})\right). \qquad (38)$$

when all the angles are mapped to the interval $(-\pi/2, \pi/2)$. We can apply the backstepping technique for discrete systems c.f. [11] to the system described by (37) and (38).

Let $f_i = -K_i(\rho_i - \rho_{\rm c})$. According to Theorem 3.3, we can select K_i such that (10) can be solved for θ_i. We let this solution be $\tilde{\theta}_i$ i.e.

$$\begin{aligned}\sin\tilde{\theta}_i &= \frac{-f_i^2 - 2\lambda_i f_i + q^2}{2\lambda_i q} \\ &= \frac{q}{2\lambda_i} - \frac{f_i}{q} - \frac{f_i^2}{2\lambda_i q}. \end{aligned} \qquad (39)$$

Using the fact that

$$f_i^2 = (\rho_{i+1} - \rho_i)^2 \ll 2(\rho_i + \frac{1}{\kappa}) = 2\lambda_i, \qquad (40)$$

we have

$$q\sin\tilde{\theta}_i = \frac{q^2}{2\lambda_i} - f_i. \qquad (41)$$

Note that $\tilde{\theta}_i$ is different from the state variable θ_i in (37) and (38). Here $\tilde{\theta}_i$ is a function of ρ_i and can be viewed as the desired value for the state θ_i.

We can then solve for the term $\frac{q^2}{2\lambda_i}$ from (41) and substitute this term in the right hand side of (37). This yields

$$\rho_{i+1} - \rho_{\rm c} = \rho_i - \rho_{\rm c} + f_i - q(\sin\theta_i - \sin\tilde{\theta}_i). \qquad (42)$$

We define

$$\tilde{\rho}_{i+1} \equiv \rho_i - \rho_{\rm c} + f_i = (1 - K_i)(\rho_i - \rho_{\rm c}). \qquad (43)$$

This $\tilde{\rho}_{i+1}$ can be viewed as the desired value for the state $\rho_{i+1} - \rho_{\rm c}$. With the help of $\tilde{\theta}_i$ and $\tilde{\rho}_{i+1}$, we rewrite (42) as

$$\rho_{i+1} - \rho_{\rm c} - \tilde{\rho}_{i+1} = -q(\sin\theta_i - \sin\tilde{\theta}_i). \qquad (44)$$

We design α_i as a feedback law so that the right hand side of (38) satisfies

$$\sin\left(\zeta_i - \varphi_i \mp (\frac{\pi}{2} - \alpha_i - \frac{\phi_i}{2})\right) = \sin\tilde{\theta}_i + \frac{\tilde{K}_i}{q}(\rho_i - \rho_{\rm c} - \tilde{\rho}_i) \qquad (45)$$

where $\tilde{K}_i$ is a scalar which will be determined later. Thus (38) becomes

$$\sin\theta_i - \sin\tilde{\theta}_i = \frac{\tilde{K}_i}{q}(\rho_i - \rho_{\rm c} - \tilde{\rho}_i). \qquad (46)$$

We show that the closed loop system given by (44) and (46) converges to the state where $\theta_i = \tilde{\theta}_i$ and $\rho_i = \rho_{\rm c}$.

Lemma 5.1: Consider the system given by (37) and (38). Let K_i and $\tilde{K}_i$ be such that $|1 - K_i| < 1$ and $|\tilde{K}_i| < 1$.

Suppose (45) has a solution for α_i. Then as $i \to \infty$, we must have $\theta_i \to \tilde{\theta}_i$ and $\rho_i \to \rho_c$.

Proof: If (45) has a solution for α_i, then (44) and (46) hold. Therefore

$$\sin\theta_i - \sin\tilde{\theta}_i = -\tilde{K}_i(\sin\theta_{i-1} - \sin\tilde{\theta}_{i-1}). \qquad (47)$$

Since $|\tilde{K}_i| < 1$, it is true that $\sin\theta_i - \sin\tilde{\theta}_i \to 0$ as $i \to \infty$. Meanwhile, from (44), we conclude $\rho_{i+1} - \rho_{\rm c} - \tilde{\rho}_{i+1} \to 0$ as $i \to \infty$. This implies that $\rho_{i+1} - \rho_{\rm c} \to (1 - K_i)(\rho_i - \rho_{\rm c})$. Since $|1 - K_i| < 1$, we conclude $\rho_i \to \rho_{\rm c}$ as $i \to \infty$. ∎

If we allow $|\tilde{K}_i|$ to be arbitrary large then (45) always has solutions for α_i. By selecting proper value for $\tilde{K}_i$, we can find a solution that satisfies the constraints for α_i. However, Lemma 5.1 requires that $|\tilde{K}_i| < 1$ to achieve asymptotic convergence. We want to find out when (45) fails to have a solution for α_i if $|\tilde{K}_i| < 1$.

If we can find $\alpha_i \in [\alpha_{\min}, \alpha_{\max}]$ such that $\sin\theta_i - \sin\tilde{\theta}_i = 0$. Then we can let $\tilde{K}_i = 0$ and a solution for α_i exists. This is exactly the inverse method.

If we can not find a constrained α_i such that $\sin\theta_i - \sin\tilde{\theta}_i = 0$, then let

$$\tilde{M}_i = \min_{\alpha_i \in [\alpha_{\min}, \alpha_{\max}]} \{|\sin\theta_i - \sin\tilde{\theta}_i|\}. \qquad (48)$$

We let

$$\tilde{K}_i = \frac{\tilde{M}_i q}{\rho_i - \rho_{\rm c} - \tilde{\rho}_i}. \qquad (49)$$

If

$$|\rho_i - \rho_{\rm c} - \tilde{\rho}_i| > \tilde{M}_i q \qquad (50)$$

is true, then $|\tilde{K}_i| < 1$. Equation (45) becomes $\sin\theta_i - \sin\tilde{\theta}_i = \tilde{M}_i$, and a solution for α_i can be found. Therefore, when a solution for α_i can not be found for $\tilde{K}_i$ given in (49), we must have

$$|\rho_i - \rho_{\rm c} - \tilde{\rho}_i| \le \tilde{M}_i q. \qquad (51)$$

We argue that this implies that the distance between the runner and the desired path becomes sufficiently small as $i \to \infty$.

We define $\tilde{M} = \sup_i \tilde{M}_i$. Since $|\sin\theta_i - \sin\tilde{\theta}_i| \le 2$ regardless of the value of θ_i and $\tilde{\theta}_i$, it is true that $\tilde{M} \le 2$. The following theorem claims that the controlled movement of the COM converges to a small neighborhood of the desired curve.

Theorem 5.2: Consider the system given by (37) and (38) controlled by the approximation method. Suppose the gain K_i is constantly K for all i and $|1 - K| < 1$. We determine the value for leg placement angle α_i by solving (45). For every i, we let $\tilde{K}_i$ be given by (49). Then we must have $\lim_{i \to \infty} |\rho_i - \rho_c| \le \tilde{M}q/(1 - |1 - K|)$.

Proof: If $|\tilde{K}_i| < 1$ for all i, Lemma 5.1 claims that the system converges to $\rho_i = \rho_{\rm c}$. Then $\lim_{i \to \infty} |\rho_i - \rho_c| = 0 < \tilde{M}q/(1 - |1 - K|)$.

If for some time indices j, $|\tilde{K}_j| \ge 1$, then condition (51) must be true. We must have

$$|\rho_j - \rho_{\rm c} - \tilde{\rho}_j| \le \tilde{M}_j q \le \tilde{M}q \qquad (52)$$

This implies that

$$|\rho_j - \rho_{\rm c}| \le |1 - K| \cdot |\rho_{j-1} - \rho_{\rm c}| + \tilde{M}q. \qquad (53)$$

For the rest of time indices i where $|\tilde{K}_i| < 1$, equation (44) implies that

$$|\rho_i - \rho_c| \le |1 - K| \cdot |\rho_{i-1} - \rho_c| + |\sin\theta_{i-1} - \sin\tilde{\theta}_{i-1}|q \quad (54)$$

Since $\tilde{K}_{i-1}$ is given by (49), We must have $|\sin\theta_{i-1} - \sin\tilde{\theta}_{i-1}| = \tilde{M}_{i-1}$. This implies that (53) is satisfied for indices i. Therefore (53) is satisfied for all i and j. Because $|1 - K| < 1$, we conclude that $\lim_{i \to \infty} |\rho_i - \rho_c| \le \tilde{M}q/(1 - |1 - K|)$. ∎

Remark 5.3: From Theorem 5.2, we conclude that larger step size (bigger q) and faster convergence rate in relative distance (bigger K) may cause larger tracking error. This agrees with intuition. The Theorem is conservative because we can make K_i adaptive. When $|\rho_i - \rho_c|$ small, we can let K_i to be close to 1 to reduce the possible tracking error. Also, $\tilde{M}$ does not have to be the supremum of $\tilde{M}_i$ for all i. Instead, we can let i be larger than any finite time. This may reduce $\tilde{M}$. Another observation is that by increasing $\alpha_{\max} - \alpha_{\min}$, we can reduce $\tilde{M}$, hence reduce the tracking error. This also agrees with intuition.

Remark 5.4: Equation (48) is used to compute α_i that minimizes the difference between θ_i and $\tilde{\theta}_i$. This is why the method is called the approximation method. Such a method can be devised heuristically without applying the backstepping technique. But the backstepping technique helps to justify convergence. One can also derive other convergent method which have different performance than the current one. But from the proof of Lemma 5.1 we conclude that the approximation method gives the fastest convergence rate among all such methods derived from the backstepping procedure.

VI. Controlled Rigid Body Dynamics

Unlike stable running along a straight line, the rigid body angular momentum p_σ should not be zero for stable running along a curve; otherwise no turning can happen. Since our goal is to control the runner to the desired curve, even if the final stable running is along a straight line, the runner need to turn in order to move to that line from an arbitrary initial position. The LLS model dynamics for the rigid body is

$$\begin{aligned} p_\sigma &= I\dot{\sigma} \\ \dot{p}_\sigma &= \tau \end{aligned} \quad (55)$$

where τ represents the torque to produce turning for the rigid body. Runners can produce this torque by using muscles connecting legs and body or by changing force distribution over multiple legs.

As indicated in Figure 9, the angle between the body axis and the velocity of the COM is $(\sigma_k - \varphi_k)$. For stable running, we want to achieve the following gaits: after the kth stance, the ending angle $(\sigma_{k+1} - \varphi_{k+1})$ differs from the starting $(\sigma_k - \varphi_k)$ only by the sign; accordingly, the direction of the angular momentum will be reversed ,i.e., $p_{\sigma_{k+1}} = -p_{\sigma_k}$.

This stable running requires that as $k \to \infty$,

$$\sigma_k - \varphi_k \to C_1 \text{ and } p_{\sigma_k} \to C_2 \quad (56)$$

for right stances and

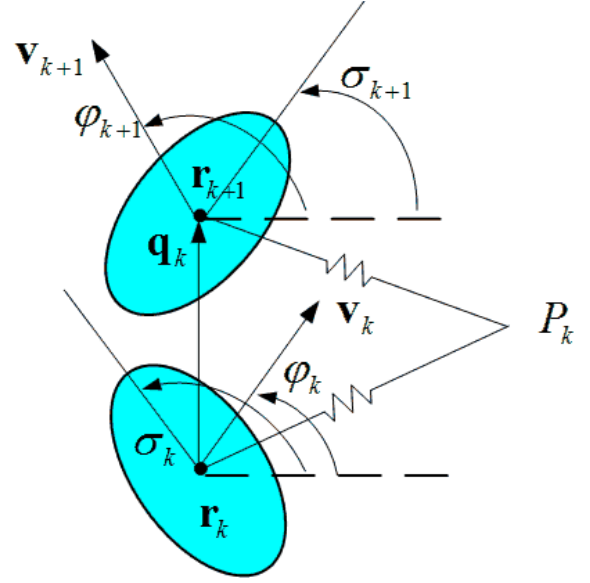$$\sigma_{k+1} - \varphi_{k+1} \to -C_1 \text{ and } p_{\sigma_{k+1}} \to -C_2 \quad (57)$$

Fig. 9. The posture of the rigid body at the beginning and the end of a stance.

for left stances where C_1 and C_2 are pre-selected constants.

For right stances, we let

$$\begin{aligned} \sigma_{k+1} - \varphi_{k+1} + C_1 &= (1 - K_4)(\sigma_k - \varphi_k - C_1) \\ p_{\sigma_{k+1}} + C_2 &= (1 - K_5)(p_{\sigma_k} - C_2) \end{aligned} \quad (58)$$

where $0 < K_4, K_5 < 1$. For left stances, we may let

$$\begin{aligned} \sigma_{k+2} - \varphi_{k+2} - C_1 &= (1 - K_4)(\sigma_{k+1} - \varphi_{k+1} + C_1) \\ p_{\sigma_{k+2}} - C_2 &= (1 - K_5)(p_{\sigma_{k+1}} + C_2). \end{aligned} \quad (59)$$

Note that φ_k and φ_{k+1} are known from (66) and (67) in Appendix I. It is not difficult to see that the discrete systems (58) and (59) achieve the desired convergence specified by (56) and (57).

Therefore, for the kth stance, we want to design the control torque τ so that starting from p_{σ_k} and σ_k, the runner will reach the state $p_{\sigma_{k+1}}$ and σ_{k+1} given by

$$\begin{aligned} p_{\sigma_{k+1}} &= (1 - K_5)p_{\sigma_k} + (2 - K_5)C_2 \\ \sigma_{k+1} &= (1 - K_4)\sigma_k + K_4\varphi_k + \\ &\quad \pi - \phi_k - 2\alpha_k + (2 - K_4)C_1. \end{aligned} \quad (60)$$

We formulate an optimal control problem with the starting state given by (p_{σ_k}, σ_k) and ending state given by $(p_{\sigma_{k+1}}, \sigma_{k+1})$ in equation (60). The ending state should be achieved within the duration T_k for the kth stance with the cost function $\int_0^{T_k} \tau^2(t)dt$ minimized. The solution for $\tau_k(t)$ for the kth stance can be obtained by applying the maximum principle. We have

$$\tau_k(t) = \frac{1}{2}\left(A_{2_k} - \frac{A_{1_k}}{I}t\right) \quad (61)$$

where $t \in [0, T_k]$, I is the moment of inertia, and

$$\begin{aligned} A_{1_k} &= \frac{24\,I^2}{T_k^3}(\sigma_{k+1} - \sigma_k) - \frac{12\,I}{T_k^2}(p_{\sigma_{k+1}} + p_{\sigma_k}) \\ A_{2_k} &= \frac{12\,I}{T_k^2}(\sigma_{k+1} - \sigma_k) - \frac{4}{T_k}p_{\sigma_{k+1}} - \frac{8}{T_k}p_{\sigma_k}. \end{aligned} \quad (62)$$

The detail of this derivation is included in Appendix II. The duration T_k can be computed in the similar way as ϕ_k in (32) as

$$T_k = 2 \int_{\eta_k}^{\eta_{\min}} \frac{1}{\sqrt{2E - \frac{p_{\psi_k}^2}{\eta^2} - 2V(\eta)}} d\eta. \qquad (63)$$

In equations (60) and (62), although $\tau_k(t)$ is open-loop control during each stance for $t \in [0, T_k]$, feedback is achieved through p_{σ_k} and σ_k when switching from one stance to another.

VII. Simulations

We present simulation results to demonstrate tracking a circle centered at the origin with radius 0.02m. The parameters for the LLS model are the same as in section V. The desired distance to the circle is 0.03m. Initially, the runner start from $(0.1, 0)$ outside the circle. The speed of the COM is 0.2m/s. The initial direction of the velocity is $\pi/3$. The leg placement angle α_i are constrained to be within the interval $(\pi/6, \pi/3)$. We change the spring constant b_k so that q_i is always equal to 1.53cm, which is 90% of the leg length at rest. The gain K_i is selected to be 0.5. When θ_i can not be achieved by α_i, we simply use the value for α_i that will minimize the differences between desired $\tilde{\theta}_i$ and achievable θ_i; hence implemented the approximation method.
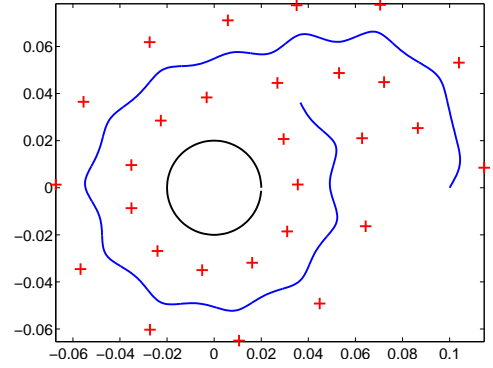
The trajectory of the COM and the distance between the COM and the circle are plotted in Figure 10. We see that the convergence is achieved after 12 stances which take less than one second.

VIII. Summary and Future Work

We have analyzed the control of LLS model and designed a hybrid curve tracking control law for legged locomotion. Using measurements of the curve for feedback, the discrete algorithm guarantees convergence to the desired curve path. During each stance, the controlled continuous dynamics is analyzed. The parameters of the LLS model is determined to implement the discrete algorithm at the beginning of each stance. We have also investigated the effects of parameter constraints. These constraints limited tracking ability. For straight lines and convex curves, a steady state can be reached. The robustness of these steady states depends on the range for the parameters.

Interesting results regarding wall following behaviors of cockroaches are reported by Camhi and Johnson in [12]. When its antenna touches the wall, a cockroach turns away from the wall but keeps the antenna in contact with the wall for a certain time period. The experiments there are performed near a raffled piecewise linear wall, not a smooth curved wall. Using a smooth curved wall with convex shape will also be interesting since a steady state can be reached.

Recently, a wall following wheeled robot using antenna like tactile sensor was reported in [8]; curve tracking for atomic force microscope is discussed in [13]; a general boundary tracking control law is derived for Newtonian particles in [14]. Our work, although intended for legged locomotion, may be adapted to handle other cases regarding curve tracking for platforms with hybrid motion dynamics.

(a) trajectory of COM
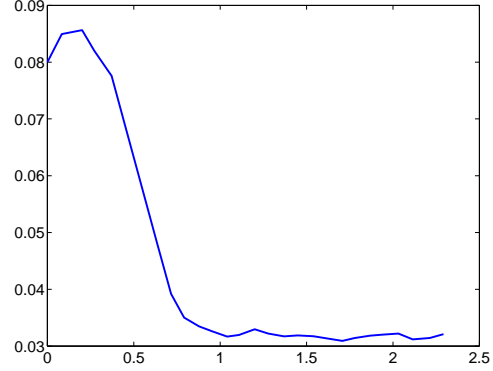
(b) distance between COM and the circle

Fig. 10. *Tracking a circle with radius* 0.02*m. In (a), the cross symbols indicate the touchdown points. The units for both horizontal and vertical axis are meters. In (b), the distance (in meters) between the COM and the circle is plotted as a function of time (in seconds). We can see it converges to the desired separation* 0.03*m.*

References

[1] R. Full and D. E. Koditschek, "Templates and anchors: Neuralmechanical hypothesis of legged locomotion on land," *Journal of Experimental Biology*, vol. 83, pp. 3325–3332, 1999.

[2] J. Schmitt and P. Holmes, "Mechanical models for insect locomotion: Dynamics and stability in the horizontal plane I. Theory," *Biological Cybernetics*, vol. 83, pp. 501–515, 2000.

[3] ——, "Mechanical models for insect locomotion: Dynamics and stability in the horizontal plane II. Applications," *Biological Cybernetics*, vol. 83, pp. 517–527, 2000.

[4] ——, "Mechanical models for insect locomotion: Stability and parameter studies," *Physica D*, vol. 156, pp. 139–168, 2001.

[5] J. Schmitt, M. Garcia, R. Razo, P. Holmes, and R. J. Full, "Dynamics and stability of legged locomotion in the horizonatoal plane: A test case using insects," *Biological Cybernetics*, vol. 86, pp. 343–353, 2002.

[6] R. M. Ghigliazza, R. Altendorfer, P. Holmes, and D. Koditschek, "A simply stablized running model," *SIAM Review*, vol. 47, no. 3, pp. 519–549, 2005.

[7] F. Zhang, A. O'Connor, D. Luebke, and P. S. Krishnaprasad, "Experimental study of curvature-based control laws for obstacle avoidance," in *Proceedings of 2004 IEEE International Conference on Robotics and Automation*, New Orleans, LA, 2004, pp. 3849–3854.

[8] A. G. Lamperski, O. Y. Loh, B. L. Kutscher, and N. J. Cowan, "Dynamical wall-following for a wheeled robot using a passive tactile sensor," in *Proc. of 2005 IEEE International Conference on Robotics and Automation*, Barcelona, Spain, 2005, pp. 3838–3843.

[9] V. Arnold, *Mathematical Methods of Classical Mechanics 2nd Ed.* New York: Springer, 1989.

[10] D. Jindrich and R. J. Full, "Many legged maneuverability: dynamics of turning in hexapods," *Journal on Experimental Biology*, vol. 202, pp. 1603–1623, 1999.

[11] R. Ordóñez and K. M. Passino, "Control of discrete time nonlinear systems with a time-varying structure," *Automatica*, vol. 39, no. 3, pp. 463–470, 2003.

[12] J. M. Camhi and E. N. Johnson, "High-frequency steering maneuvers mediated by tactile cues: Antennal wall-following in the cockroach," *Journal of Experimental Biology*, vol. 202, pp. 631–643, 1999.

[13] S. B. Andersson and J. Park, "Tip steering for fast imaging in AFM," in *Proceedings of 2005 American Control Conference*, Portland, OR, June 6-10, 2005, pp. 2469–2474.

[14] F. Zhang, E. Justh, and P. S. Krishnaprasad, "Boundary following using gyroscopic control," in *Proc. of 43rd IEEE Conference on Decision and Control*, Atlantis, Paradise Island, Bahamas, 2004, pp. 5204–5209.

APPENDIX I
DISCRETE DYNAMICS FOR LEG PARAMETERS

The feasible θ_k and θ_{k+1} that can be generated from the LLS model parameters must satisfies (28) and (29). Equation (28) subtract (29) yields

$$\theta_{k+1} - \theta_k = (\zeta_{k+1} - \varphi_{k+1}) - (\zeta_k - \varphi_k) + \pi - (\alpha_k + \alpha_{k+1}) - \frac{\phi_k + \phi_{k+1}}{2}. \quad (64)$$

The angle $(\zeta_k - \varphi_k)$ is measured between the COM velocity vector and the tangent vector of the desired curve. In a similar fashion, we find

$$\theta_{k+2} - \theta_{k+1} = (\zeta_{k+2} - \varphi_{k+2}) - (\zeta_{k+1} - \varphi_{k+1}) - \pi + (\alpha_{k+2} + \alpha_{k+1}) + \frac{\phi_{k+2} + \phi_{k+1}}{2}. \quad (65)$$

We now establish a difference equation which describes the change of $(\zeta_k - \varphi_k)$.

Comparing the COM velocity $\mathbf{v}_k$ and $\mathbf{v}_{k+1}$, we notice that they are reflectively symmetric to each other with $\mathbf{q}_k$ as the axis of symmetry, as shown in Figure 7. This can be proved from the solution of equations (26). From Figure 3, we conclude that

$$\varphi_{k+1} - \varphi_k = 2(\frac{\pi}{2} - \frac{\phi_k}{2} - \alpha_k) \quad (66)$$

from a right stance to a left stance and

$$\varphi_{k+2} - \varphi_{k+1} = -2(\frac{\pi}{2} - \frac{\phi_{k+1}}{2} - \alpha_{k+1}) \quad (67)$$

from a left stance to a right stance. From Figure 2, we can derive the change of ζ_k as

$$\zeta_{k+1} - \zeta_k = \gamma_k. \quad (68)$$

The angle γ_k can be determined using the sine law

$$\frac{\sin \gamma_k}{q_k} = \frac{\sin \beta}{\rho_{k+1} + \frac{1}{\kappa}}. \quad (69)$$

We use $\beta = \pi/2 - \theta_k$ and $\rho_{k+1} = \rho_k + f_k$ to obtain

$$\sin \gamma_k = \frac{q_k}{\lambda_k + f_k} \cos \theta_k. \quad (70)$$

From (66) and (68), we obtain

$$(\zeta_{k+1} - \varphi_{k+1}) - (\zeta_k - \varphi_k) = \gamma_k - (\pi - \phi_k - 2\alpha_k). \quad (71)$$

Similarly,

$$(\zeta_{k+2} - \varphi_{k+2}) - (\zeta_{k+1} - \varphi_{k+1}) = \gamma_{k+1} + (\pi - \phi_{k+1} - 2\alpha_{k+1}). \quad (72)$$

Using (71) and (64), we deduce that

$$\theta_{k+1} - \theta_k = -(\alpha_{k+1} - \alpha_k) - \frac{\phi_{k+1} - \phi_k}{2} + \gamma_k. \quad (73)$$

Using (72) and (65), we have

$$\theta_{k+2} - \theta_{k+1} = (\alpha_{k+2} - \alpha_{k+1}) + \frac{\phi_{k+2} - \phi_{k+1}}{2} + \gamma_{k+1}. \quad (74)$$

Equations (73) and (74) must be satisfied for all feasible θ_k, θ_{k+1}, and θ_{k+2}.

APPENDIX II
OPTIMAL CONTROL FOR RIGID BODY DYNAMICS

The system equations for the rigid body dynamics is

$$\begin{aligned} \dot{\sigma} &= \frac{p_\sigma}{I} \\ \dot{p}_\sigma &= \tau. \end{aligned} \quad (75)$$

We want to minimize the cost function $\int_0^{T_k} \tau^2(t)dt$. Applying the maximum principle, we define the controlled Hamiltonian as

$$\begin{aligned} H_{\lambda,\tau} &= \lambda_1 \dot{\sigma} + \lambda_2 \dot{p}_\sigma - \tau^2 \\ &= \lambda_1 \frac{p_\sigma}{I} + \lambda_2 \tau - \tau^2 \end{aligned} \quad (76)$$

where λ_1 and λ_2 are the adjoint variables. The optimal control τ that minimizes $H_{\lambda,\tau}$ is computed by letting $\partial H_{\lambda,\tau}/\partial \tau = 0$. This yields $\tau = \lambda_2/2$. The Hamiltonian for the system under this control is

$$H_\lambda = \lambda_1 \frac{p_\sigma}{I} + \frac{1}{4}\lambda_2^2. \quad (77)$$

This Hamiltonian induces the following Hamilton's equations:

$$\begin{aligned} \dot{\sigma} &= \frac{p_\sigma}{I} \\ \dot{p}_\sigma &= \frac{\lambda_2}{2} \\ \dot{\lambda}_1 &= 0 \\ \dot{\lambda}_2 &= -\frac{1}{I}\lambda_1. \end{aligned} \quad (78)$$

From these equations we first observe that $\lambda_1(t) = \lambda_1(0)$. Then we can solve for λ_2 as

$$\lambda_2(t) = \lambda_2(0) - \frac{\lambda_1(0)}{I}t. \quad (79)$$

In order to determine $\lambda_1(0)$ and $\lambda_2(0)$, we integrate

$$\dot{p}_\sigma = \frac{1}{2}(\lambda_2(0) - \frac{\lambda_1(0)}{I}t) \quad (80)$$

from 0 to T_k. This yields

$$p_{\sigma_{k+1}} = p_{\sigma_k} + \frac{1}{2}\lambda_2(0)T_k - \frac{1}{4}\frac{\lambda_1(0)}{I}T_k^2. \quad (81)$$

We then integrate

$$\dot{\sigma} = \frac{p_\sigma}{I} = \frac{1}{I}\left(p_{\sigma_k} + \frac{1}{2}\lambda_2(0)t - \frac{1}{4}\frac{\lambda_1(0)}{I}t^2\right). \quad (82)$$

This gives us

$$\sigma_{k+1} = \sigma_k + \frac{1}{I}p_{\sigma_k}T_k + \frac{1}{4I}\lambda_2(0)T_k^2 - \frac{1}{12I^2}\lambda_1(0)T_k^3. \quad (83)$$

From (81) and (83) we can solve for $\lambda_1(0)$ and $\lambda_2(0)$. One can verify that $\lambda_1(0) = A_{1_k}$ and $\lambda_2(0) = A_{2_k}$, where A_{1_k} and A_{2_k} are given in (62), are the solutions.